

ELECTRON TUNNELING AND CONTACT RESISTANCE OF METAL-SILICON CONTACT BARRIERS*

A. Y. C. YU

Fairchild Semiconductor, Research and Development Laboratory,
Palo Alto, California 94304, U.S.A.

(Received 20 February 1969; in revised form 17 April 1969)

Abstract—The contact resistance of Al and Pt on *n*-type Si over a wide range of doping concentrations ($10^{18} \rightarrow 2 \times 10^{20} \text{ cm}^{-3}$) has been measured at both room temperature and liquid nitrogen temperature. These experimental results are compared with theoretical calculations based on a model with electron tunneling through the potential barrier at the interface as the dominant mechanism of current flow. Good agreement is found. It is hoped that this physical model can be used as a guideline in developing ohmic contacts for various semiconductor devices.

Résumé—La résistance de contact de Al et de Pt sur du Si du type-*n* sur une gamme étendue de concentration de doping ($10^{18} \rightarrow 2 \times 10^{20} \text{ cm}^{-3}$) a été mesurée à la température ambiante et à la température de l'azote liquéfié. Ces résultats expérimentaux sont comparés aux calculs théoriques fondés sur un modèle ayant un tunnel d'électrons à travers la barrière de potentiel à l'interface comme mécanisme dominant d'écoulement de courant. On espère que ce modèle physique pourra être utilisé comme guide pour le développement de contacts ohmiques pour divers dispositifs à semiconducteurs.

Zusammenfassung—Der Übergangswiderstand von Al und Pt auf *n*-Type Si ist über einen weiten Bereich von Dotierungskonzentrationen ($10^{18} \rightarrow 2 \times 10^{20} \text{ cm}^{-3}$) sowohl bei Raumtemperatur wie bei flüssiger Stickstofftemperatur gemessen worden. Diese experimentellen Ergebnisse werden mit theoretischen Berechnungen verglichen, die sich auf ein Modell mit Elektronentunnel durch den Potentialwall an der Grenzschicht als vorwiegender Mechanismus des Stromflusses basieren. Eine gute Übereinstimmung wird gefunden. Man hofft, dass dieses physikalische Modell als Führer im Entwickeln von ohmischen Kontakten für verschiedene Halbleitervorrichtungen benutzt werden kann.

1. INTRODUCTION

METAL-SEMICONDUCTOR (M-S) contacts can be divided into two groups: those made on lightly doped semiconductors and those made on heavily doped semiconductors. The first, commonly called Schottky barriers, have been extensively studied and thermionic emission has been established as the mechanism of current flow. Recent advances such as the incorporation of *p-n* junction guard rings^(1,2) and surface effect studies⁽³⁾ now make possible the fabrication of stable Schottky barrier diodes with near-ideal characteristics.

Ohmic contacts, which are usually made by metals on heavily doped semiconductors, are of great importance since they are an essential part of all solid-state devices. Yet, there is no general agreement about their physical nature. Although there is a wealth of experimental data in the literature on ohmic contacts, different fabrication methods and measuring techniques make it difficult to compare and analyze them. Therefore, we have made metal contacts (Al and Pt) on *n*-type silicon over a wide range of doping concentration ($10^{18} \rightarrow 2 \times 10^{20} \text{ cm}^{-3}$) under similar fabricating conditions and studied their contact resistance systematically. These data can be satisfactorily explained by a simple physical

* A preliminary form of this paper was presented at the IEEE International Electron Devices Meeting, Washington, D.C., October 1968.

model with electron tunneling through the potential barrier at the contact interface as the dominant mechanism of current flow.

The theoretical considerations are presented in Section 2 of this paper. Methods of contact resistance measurements and contact fabrication (Section 3) are then discussed. Comparison and discussion of experimental data and theoretical calculations follow (Section 4). Finally, conclusions are summarized (Section 5).

2. THEORY

If an M-S contact has no potential barrier at the interface, a true ohmic results which has a linear current-voltage characteristic and its resistance is just that of the bulk semiconductor. However, M-S contacts can appear ohmic for other reasons as well. If the potential barrier is so low that a negligible amount of voltage drops across the interface, again an ohmic behavior is observed (e.g., Au and Pt on *p*-type Si). However, practical ohmic contacts on *n*-type Si are made by metals such as Al, Au, and Pt, which are known to form fairly high barriers (0.7–0.9 eV) on lightly doped Si. Since it is also known that the barrier height is essentially independent of the semiconductor doping concentration⁽⁴⁾ (except for image force lowering which should be less than 0.2 eV for $N_D \leq 10^{20} \text{ cm}^{-3}$), it is clear that relatively high barriers (> 0.5 eV) exist in such contacts on heavily doped silicon. Therefore, these contacts are ohmic for a different reason.

When the doping concentration is high, the depletion region width becomes small. Therefore, electrons can easily tunnel through the barrier, in addition to the thermionic emission process. This added component of current reduces the voltage drop across the contact such that most of the applied voltage is dropped across the semiconductor bulk. Thus the terminal current-voltage characteristic of such a contact is ohmic. This model was first pointed out by KRÖGER *et al.*⁽⁵⁾ and subsequently pursued by others.^(6–8) We shall show later (Section 4) that this is indeed the correct physical picture of metal-*n*Si contacts when the doping is heavy. Electron tunneling in M-S contacts on heavily doped III-V semiconductor compounds has recently received a great deal of attention.^(9–16) Some of the relevant theoretical considerations are discussed below.

In Fig. 1, band diagrams of forward biased M-S contacts are shown. Figure 1(a) depicts the situation where the semiconductor is lightly doped. In this case, the depletion width is so wide that the only way the electrons can get into the metal is by thermionic emission over the potential barrier ϕ_B .

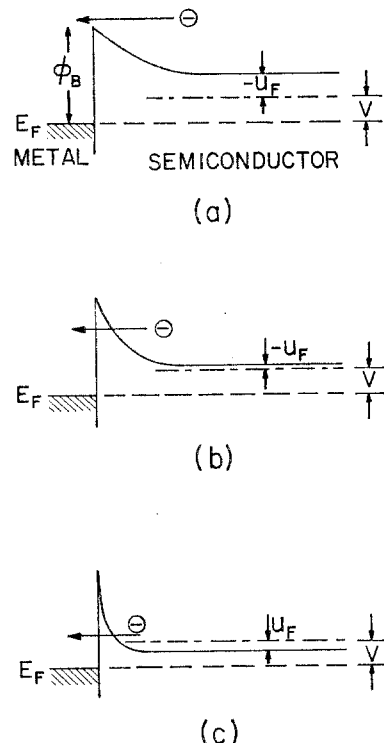


FIG. 1 Band diagrams of metal *n*-type semiconductor contacts under forward bias voltage: (a) semiconductor lightly doped, $kT/E_{00} \gg 1$, (b) semiconductor heavily doped, $kT/E_{00} \sim 1$, (c) semiconductor very heavily doped (degenerate), $kT/E_{00} \ll 1$.

A useful characteristic energy E_{00} is defined as⁽⁹⁾

$$E_{00} = \frac{q\hbar}{2\sqrt{\left(\frac{N_D}{m^*\epsilon}\right)}} \quad (1)$$

where q is the electronic charge, \hbar is Planck's constant, N_D is the donor concentration, m^* is the effective mass of the tunneling electron, and ϵ is the dielectric constant of the semiconductor. A plot of E_{00} as a function of N_D is shown in Fig. 2, where m is the free electron mass and ϵ_0 is the permittivity of free space. This

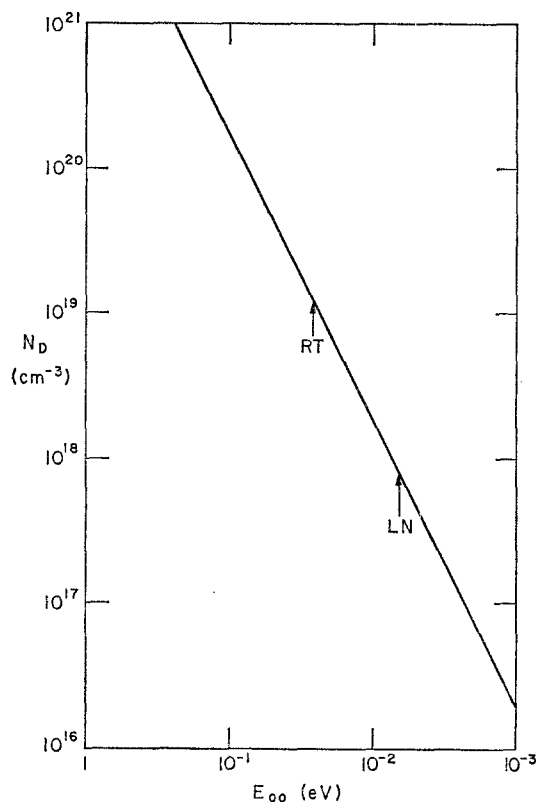


FIG. 2. Plot of E_{00} as a function of N_D with $m^*/m = 0.5$
 $\epsilon/\epsilon_0 = 12$.

energy is related to the tunneling probability and E_{00} increase with N_D since the depletion region width decreases which makes the potential barrier thinner and easier to tunnel through. Therefore, the ratio kT/E_{00} is a measure of the relative importance of the thermionic process in relation to the tunneling process. For lightly doped semiconductors, it is clear that $kT/E_{00} \gg 1$ [Fig. 1(a)]. Figure 1(b) shows the band diagram of an M-S contact on a heavily doped semiconductor. In this case, the thermionic and tunneling processes are comparable ($kT/E_{00} \approx 1$) and the dominant mechanism of current flow is due to electrons with some thermal energy tunneling through the midsection of the potential barrier. This is commonly called the thermionic-field-emission (TFE).^(9,15) When the semiconductor is very heavily doped or at very low temperature ($kT/E_{00} \ll 1$), the current is carried by electrons tunneling from the Fermi level in the semicon-

ductor into the metal. This process is called field-emission (FE).^(9,15)

Theoretical calculations of current-voltage characteristics in the tunneling region based on the simple band model shown in Fig. 1 have been done either exactly⁽¹⁰⁾ or by using the WKB approximation.^(12,15,16) Since the latter approach yields relatively simple analytical results which are quantitatively similar to the exact calculation, these results will be used here.

In the FE region, the specific contact resistance R_c ($\Omega \cdot \text{cm}^2$) is easily calculated from theoretical (WKB approximation) V-I characteristics.⁽¹⁶⁾ The result is

$$R_c \equiv \left. \frac{dV}{dJ} \right|_{V \rightarrow 0} = \left[\frac{A\pi q}{kT \sin(\pi c_1 kT)} \exp\left(\frac{-\phi_B}{E_{00}}\right) - \frac{Ac_1 q}{(c_1 kT)^2} \exp\left(\frac{-\phi_B}{E_{00}} - c_1 u_F\right) \right]^{-1} \quad (2)$$

where

$$A = \frac{4\pi m^* q (kT)^2}{h^3}, \quad (3)$$

is the Richardson constant times T^2 .[†]

The above equation is valid if

$$1 - c_1 kT > kT(\sqrt{2}f_1). \quad (4)$$

And if $\phi_B \gg u_F$, simple expressions for c_1 and f_1 can be obtained.

$$c_1 = \frac{1}{2E_{00}} \ln \left[\frac{4\phi_B}{u_F} \right], \quad (5)$$

$$f_1 = \frac{1}{4E_{00}u_F}. \quad (6)$$

For barriers (> 0.5 eV) on n -Si, this equation is valid at room temperature if $N_D \geq 10^{20} \text{ cm}^{-3}$, and at liquid nitrogen temperature if $N_D > 5 \times 10^{19} \text{ cm}^{-3}$. Below these concentrations, TFE is important. Similarly, the specific contact resistance in the TFE range can be calculated and is found

[†] It should be noted that the effective mass m^* here should be different from that in (1). However, in this simple model, they are taken to be equal for simplicity.

to be^(15,16)

$$R_c \equiv \frac{dV}{dJ} \Big|_{V \rightarrow 0} = \left[\frac{kT}{qA} \right] \frac{kT}{[\sqrt{\pi(\phi_B + u_F)} E_{00}]} \times \cosh\left(\frac{E_{00}}{kT}\right) \left[\sqrt{\coth\left(\frac{E_{00}}{kT}\right)} \right] \times \exp\left[\frac{\phi_B + u_F}{E_0} - \frac{u_F}{kT}\right], \quad (7)$$

where

$$E_0 = E_{00} \coth\left(\frac{E_{00}}{kT}\right). \quad (8)$$

Equation (7) is valid if

$$\frac{\cosh^2\left(\frac{E_{00}}{kT}\right)}{\sinh^3\left(\frac{E_{00}}{kT}\right)} < \frac{2(\phi_B + u_F)}{3E_{00}}. \quad (9)$$

E_0 is a measure of tunneling probability in the TFE region.

In the thermionic emission (TE) range when $kT/E_{00} \gg 1$, the specific contact resistance is given by

$$R_c = \frac{dV}{dJ} \Big|_{V \rightarrow 0} = \frac{kT}{qA} \exp\left(\frac{\phi_B}{kT}\right). \quad (10)$$

A closer examination of these results is warranted. The functional dependence of the contact resistance on semiconductor doping level [Equations (2), (7), and (10)] can be written as

$$\exp\left[\frac{\phi_B}{\sqrt{N_D}}\right] \quad \text{FE(if } c_1 u_F \gg 1\text{), (11)}$$

$$\exp\left[\frac{\phi_B}{(\sqrt{N_D}) \coth\left(\frac{E_{00}}{kT}\right)}\right] \quad \text{TFE, (12)}$$

$$\exp\left[\frac{\phi_B}{kT}\right] \quad \text{TE. (13)}$$

Figure 3 depicts the expected functional form of $\ln R_c$ plotted vs $1/\sqrt{N_D}$. In the FE region, $\ln R_c$ depends linearly on $1/\sqrt{N_D}$ with slope

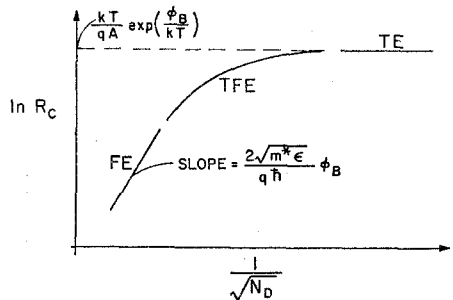


FIG. 3. Theoretical dependence of the specific contact resistance on the doping concentration.

$[2(\sqrt{m^*}\epsilon)/q\hbar]\phi_B$, since the tunneling probability has this dependence. In the TE regions, R_c is independent of the doping concentration and is equal to $(kT/qA) \exp(\phi_B/kT)$ since the thickness of the barrier has little bearing on the thermionic emission process (assuming, of course, that the barrier is not too thick to have scattering of electrons in this region). The TFE region bridges the two. We shall show in Section 4 that the observed specific contact resistance does agree with the theoretical calculation, thus confirming the tunnel model discussed in this section.

3. EXPERIMENTAL METHODS

(a) Method of contact resistance measurement

When the contact resistance is much larger than the series bulk resistance, it can be easily measured either by examining the V-I characteristic of a simple diode structure on a curve tracer or by using a lock-in amplifier to measure the small-signal ac current with a small a.c. voltage (≤ 10 mV) applied to the diode at zero d.c. bias. When the contact resistance is comparable to the bulk resistance, these techniques are clearly inadequate. We employed a technique due to SHOCKLEY⁽¹⁷⁾ which is illustrated in Fig. 4. A thin n -layer is first diffused into a p -substrate. Then a thin strip is isolated by etching and a metal-pattern is deposited (shaded regions). Two probes are used to send a current I through the strip while the voltage across two other probes is measured. A plot of this voltage as a function of distance yields a transfer length L_t , as shown in Fig. 4(c). The contact resistance is related to L_t and the sheet resistivity R_s of the diffused layer (R_s is determined by

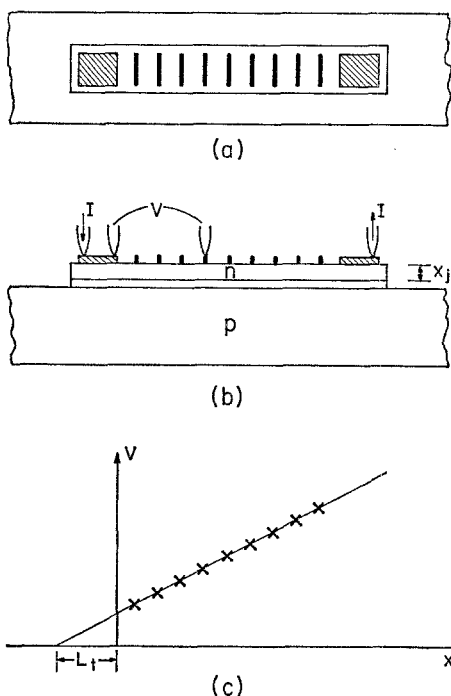


FIG. 4. Shockley's scheme of contact resistance measurement: (a) top view, (b) side view, (c) determination of L_t .

usual four point probe measurement) by⁽¹⁷⁾

$$R_c = R_s L_t^2 \quad (14)$$

A special probing station made by W. W. Hooper was used in these measurements. Typical data are shown in Fig. 5.

(b) *Contact fabrication*

Two types of M-S contacts were made on *n*-type Si. The first type is a simple diode structure as shown in Fig. 6, made on uniformly phosphorus

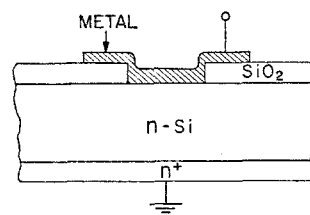


FIG. 6. Simple diode structure.

doped $\langle 111 \rangle$ Si wafers (150μ thick) with $N_D \leq 5 \times 10^{18} \text{ cm}^{-3}$. The series bulk resistance of these diodes is small compared to that of the contact. The surface concentration is obtained

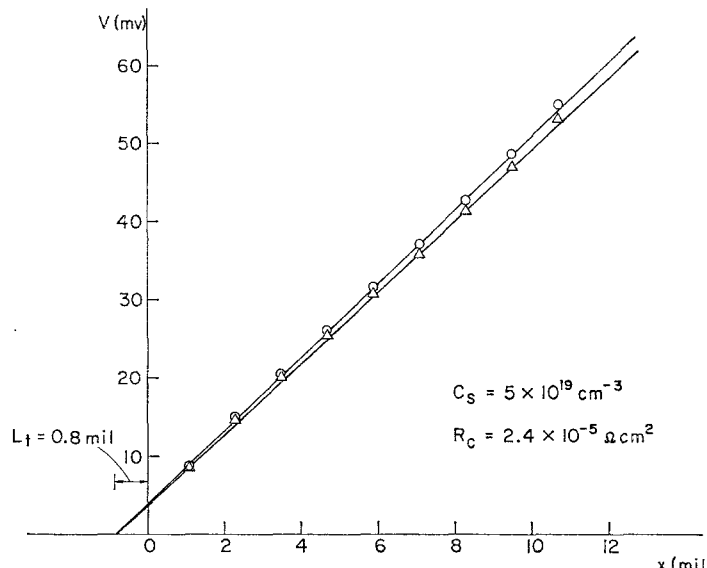


FIG. 5. Typical experimental data of contact resistance measurement using Shockley's scheme on Al-*n*Si contact ($I = 5 \text{ mA}$). Two symbols denote two different contacts on the same wafer.

from measured resistivity values^(18,19) and the slope of the C-V plot.⁽²⁰⁾ An n^+ layer with surface concentration $\sim 2 \times 10^{20} \text{ cm}^{-3}$ is diffused into the back to ensure a low contact resistance on the back side.

The second type of contact is made on phosphorus diffused layers as shown in Fig. 4. These layers are first predeposited with phosphorus and then diffused at 1200°C in dry oxygen for different lengths of time to produce surface concentrations in the range 3.5×10^{19} to $2.0 \times 10^{20} \text{ cm}^{-3}$. This diffusion schedule is chosen so that redistribution at the surface is negligible.⁽²¹⁾ This is essential since it is the surface concentration that is of importance. The junction depth x_j and the sheet resistivity R_s were measured after diffusion. Assuming a Gaussian distribution of phosphorus atoms, the surface concentration can be calculated from known x_j and R_s .⁽¹⁸⁾

Both Al and Pt were used in making these contacts since they are commonly used in making ohmic contacts on Si devices. Evaporations were done by electron-beam gun in typical pressure of 10^{-6} Torr in an oil diffusion pump with a liquid nitrogen-cooled trap. Prior to Al deposition ($\sim 1 \mu$), Si wafers were first dipped in 10:1 HF to remove any residual oxide and then quenched in methanol. After evaporation, the pattern was defined by the usual photoresist technique. Annealing in dry N_2 at 400–500°C does not change the measured resistance values. Prior to Pt deposition, the wafers were heated to 400°C in the vacuum system and held at this temperature during Pt evaporation, forming Pt-silicide at the contact.⁽²²⁾ To avoid etching, a lifting technique was used to define the geometry.⁽⁸⁾ Room-temperature measurements were done by wafer probing. The wafers were then scribed and individual die

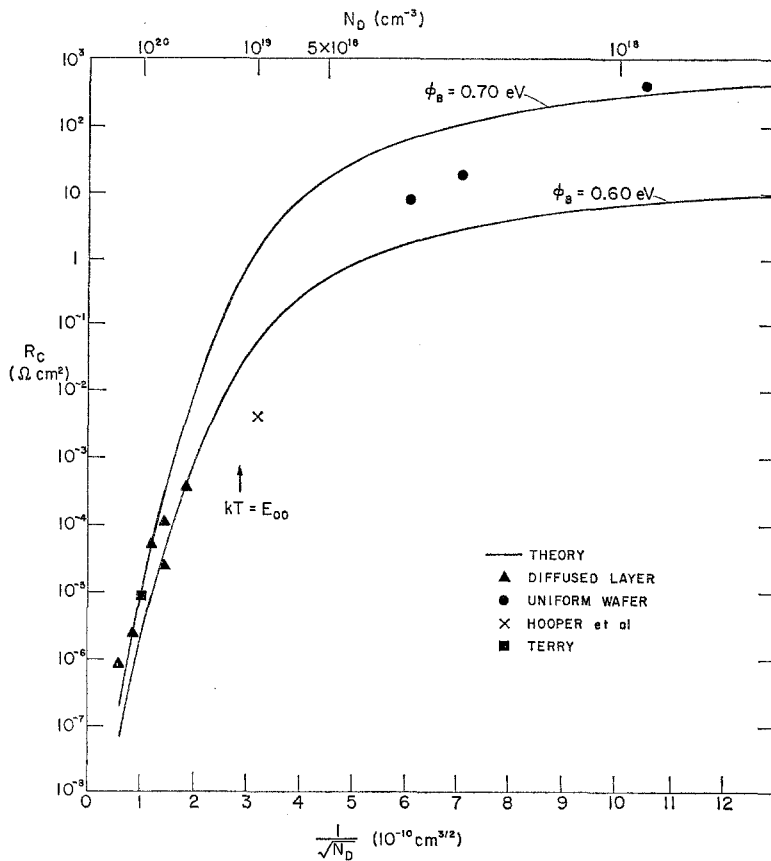


FIG. 7. Plot of $\ln R_c$ vs. $1/\sqrt{N_D}$ for Al- n Si contact at room temperature.

were mounted in transistor headers for liquid nitrogen temperature measurements.

4. DISCUSSION OF EXPERIMENTAL AND THEORETICAL RESULTS

Figures 7 and 8 show plots of $\ln R_c$ as a function of $1/\sqrt{N_D}$ for Al-nSi contacts and Pt-nSi contacts at room temperature. The lines are theoretical calculations from (2), (7), and (10), with $m^*/m = 0.5$ and $\phi_B = 0.60$ eV and 0.70 eV.[†] In Fig. 7, in addition to our data in triangles and circles, other

[†]The effective mass of electrons in the <111> direction of Si should be 0.25.⁽²³⁾ However, if this value is used, the theoretical results are slightly lower than the experimental data. It is conceivable that impurity band merging with the conduction band at $N_D \geq 2 \times 10^{19} \text{ cm}^{-3}$ could have bearing on this point.⁽²⁴⁾ However, for our present purpose, m^* is considered as a parameter.

published^(25,26) data are included as well, and the agreement is satisfactory.

It is clear from examining these figures that the experimental data agree well with the theoretical predictions. In the high doping range ($> 10^{19} \text{ cm}^{-3}$) R_c is a sensitive function of N_D and the $\ln R_c$ vs. $1/\sqrt{N_D}$ plot is almost a straight line, as expected (Section 2). It is interesting to note that the contact resistances of Al and Pt contacts are very similar in this range. As the doping concentration is reduced, R_c tends to bend over and eventually saturates as N_D approaches 10^{17} cm^{-3} .

Since TFE is much more temperature-sensitive than FE, it is expected that the contact resistance of M-S contacts on less heavily doped samples will increase manyfold as the temperature is reduced, while that on the more heavily doped samples will hardly change. Figure 9 shows the experimental

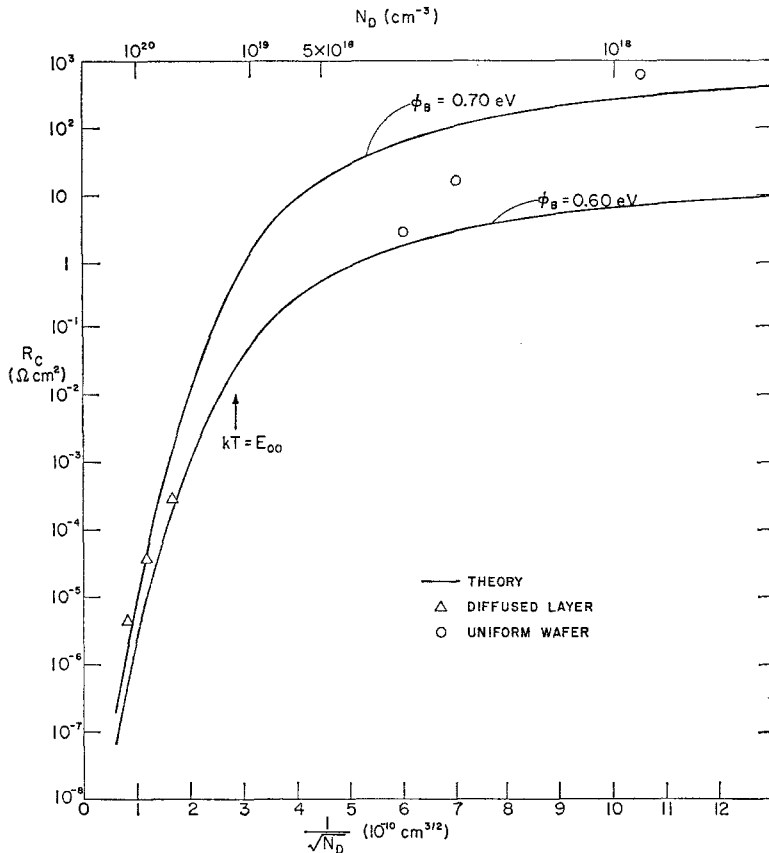


FIG. 8. Plot of $\ln R_c$ vs. $1/\sqrt{N_D}$ for Pt-nSi contacts at room temperature.

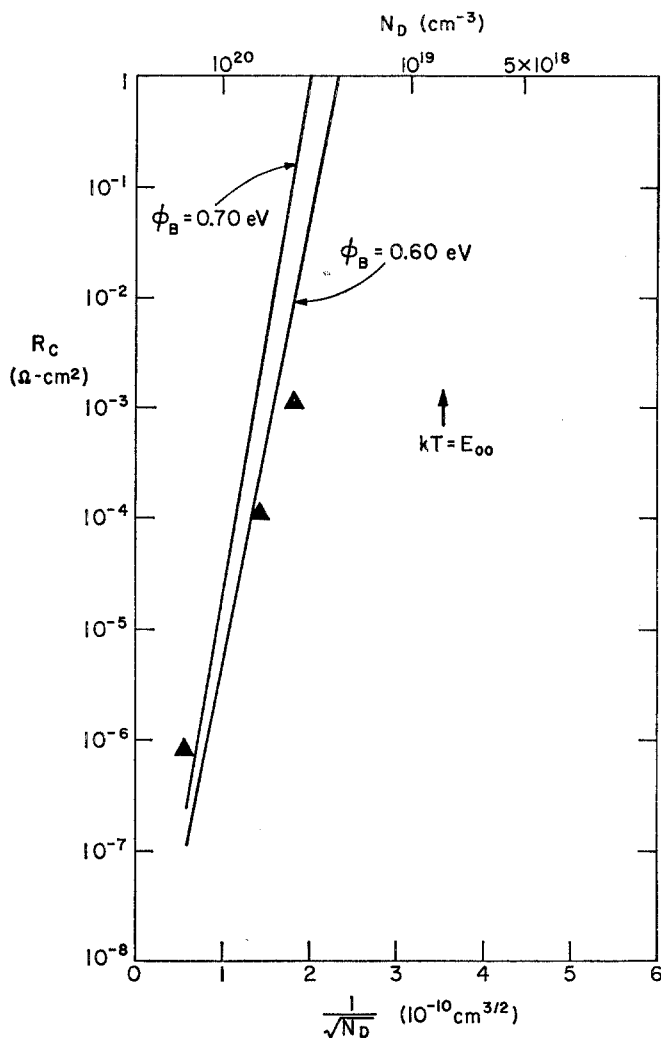


FIG. 9. Plot of $\ln R_c$ vs. $1/\sqrt{N_D}$ for Al-*n*Si contacts at liquid nitrogen temperature.

data and theoretical calculation at liquid nitrogen temperature. It is clear that the agreement is good in the degenerate region. All the diodes made on uniformly doped wafers ($N_D < 5 \times 10^{18} \text{ cm}^{-3}$) have very high contact resistance ($> 10^3 \Omega\text{-cm}^2$, which is the upper limit of the measuring equipment) at liquid nitrogen temperature. These data, because they are not available, are not shown.

It should be pointed out that although the qualitative dependence of R_c on N_D is in agreement with the theoretical prediction, the good quantitative agreement may be fortuitous for the following

reasons. The effective mass value has been used as a parameter. Image force lowering, the effects of impurity bands, the possibility of tunneling through traps and the use of two-band model instead of the one-band model have not been considered. However, inclusion of these additional effects can only obscure the physical picture at this time. Therefore, we have only compared our experimental data with the simplest theoretical model.

5. CONCLUSIONS

We have measured the contact resistance

$(dV/dJ|_{V \rightarrow 0})$ of Al and Pt contacts on n -Si over a wide range of silicon doping concentrations ($10^{18} \rightarrow 2 \times 10^{20} \text{ cm}^{-3}$). We have shown that these data are consistent with a model with electron tunneling through the potential barrier at the contact interface as the dominant mechanism of current flow. This is in agreement with prior experimental results on Ge⁽⁸⁾ and GaAs.⁽⁶⁾ It can be concluded that the tunneling model is applicable to a large number of ohmic contact systems on solid state devices.

It is hoped that this physical model can be used as a guideline in developing ohmic contacts for various semiconductor devices.

Acknowledgements—The author is grateful to C. A. MEAD, W. W. HOOPER, E. H. SNOW, R. J. WHITTIER and F. A. PADOVANI for helpful suggestions and discussions; C. A. MEAD, F. A. PADOVANI, C. R. CROWELL and L. E. TERRY for communicating their useful results prior to publication; and D. SANDAGE and A. MELGER for their technical assistance.

REFERENCES

1. M. P. LEPSALTER and S. M. SZE, *Bell Syst. tech. J.* **47**, 195 (1968).
2. R. A. ZETTLER and A. M. COWLEY, *IEEE Trans. Electron Devices*, **16**, 58 (1968).
3. A. Y. C. YU and E. H. SNOW, *J. appl. Phys.* **39**, 3008 (1968).
4. D. KAHNG, *Solid-St. Electron.* **6**, 281 (1863).
5. F. A. KROGER, G. DIEMER and H. A. KLASSENS, *Phys. Rev.* **103**, 279 (1956).
6. C. A. MEAD, "Ohmic contacts to semiconductors," Electrochemical Society, New York (1969).
7. J. VILMS and L. WANDINGER, "Ohmic contacts to semiconductors," Electrochemical Society, New York (1969).
8. J. W. CONLEY and J. J. TIEMANN, *J. appl. Phys.* **38**, 2880 (1967).
9. F. A. PADOVANI and R. STRATTON, *Solid-St. Electron.* **9**, 695 (1966).
10. J. W. CONLEY, C. B. DUKE, G. D. MAHAN and J. J. TIEMANN, *Phys. Rev.* **150**, 466 (1966).
11. J. W. CONLEY and G. D. MAHAN, *Phys. Rev.* **161**, 681 (1967).
12. R. STRATTON and F. A. PADOVANI, *Solid-St. Electron.* **10**, 813 (1967).
13. G. H. PARKER and C. A. MEAD, *Phys. Rev. Lett.* **21**, 605 (1968).
14. M. F. MILLEA, M. McCALL and C. A. MEAD, *Phys. Rev.* **177**, 1164 (1969).
15. C. R. CROWELL and V. L. RIDEOUT, *Solid-St. Electron.* **12**, 89 (1969).
16. F. A. PADOVANI (to be published).
17. W. SHOCKLEY, in "Research and Investigation of Inverse Epitaxial UHF Power Transistor," Final Technical Report No. AL-TDR-64-207, September 1964, Air Force Atomic Laboratory, Air Force Systems Command, Wright-Patterson Air Force Base, Ohio.
18. A. S. GROVE, *Physics and Technology of Semiconductor Devices*, Wiley, New York (1967).
19. J. C. IRVIN, *Bell Syst. tech. J.* **41**, 387 (1962).
20. C. A. MEAD, *Solid-St. Electron.* **9**, 1023 (1966).
21. A. S. GROVE, O. LEISTIKO, JR. and C. T. SAH, *J. appl. Phys.* **35**, 2695 (1964).
22. D. KAHNG and M. P. LEPSALTER, *Bell Syst. tech. J.* **44**, 1525 (1966).
23. C. R. CROWELL, *Solid-St. Electron.* **12**, 55 (1969).
24. M. N. ALEXANDER and D. F. HOLCOMB, *Rev. Mod. Phys.* **40**, 815 (1968).
25. R. C. HOOPER, J. A. CUNNINGHAM and J. G. HARPER, *Solid-St. Electron.* **8**, 831 (1965).
26. L. E. TERRY, "Ohmic contacts to semiconductors," Electrochemical Society, New York (1969).